

# Empirical Relationships between Hardness, Replica and Strain and Their Roles in Health Monitoring based Life Assessment for Aged Power Plant Materials

R. Bonetti<sup>a</sup>, A. Morris<sup>b</sup>, P.H. Shipway<sup>a</sup>, W. Sun<sup>a</sup>

<sup>a</sup> Faculty of Engineering, University of Nottingham, Nottingham NG7 2RD UK

<sup>b</sup> EDF Energy (UK), Coal and Gas Operations, Central Technical Organisation, Barnwood, Gloucester GL4 3RS UK

## ABSTRACT

In this paper, for the first time, a holistic empirical lifing approach, which accommodates the on-site information of replica, hardness and strain, is established based on a large amount of outage inspection data on ageing high temperature parent  $\frac{1}{2}\text{Cr}\frac{1}{2}\text{Mo}\frac{1}{4}\text{V}$  (CrMoV) material and has been used to illustrate how such routinely collected inspection data can be better utilised to provide the plant operator with predictions of residual creep life. The model differentiates between long term and persistent thermal softening behaviour revealed by change in hardness over time and short-term creep cavitation that accelerates material damage. Importantly the models developed are designed to be used iteratively with surface replica and hardness data available from an outage inspection. The study shows that the availability of more data will enable further refinements, but more importantly it emphasises the importance of systematically capturing this data and processing at the time of inspection to forecast residual life and then updating and tuning the model periodically at future inspections. The capture of strain data from pipe diametral measurements is also a routine outage activity and this data is included in the case study to demonstrate the capabilities in the residual life forecast by the new methods.

## KEYWORDS

Creep life, hardness, replica, health monitoring, rate of change, power plant data, CrMoV steels

## Nomenclature

$A_0$	Constant in the Failure Forecast method
$A_1$	Constant in the Masuyama hardness drop relationship
$A_2$	Factor in the Arrhenius function
$A$	Parameter in the Shammass equation
$a, b$	Constants in the hardness-minimum creep rate relationship by Morris et al. [1]
$b_1$	Burgers vector
$B$	Constant in the creep rupture equation
$cavities_{max}$	Max acceptable cavities
$HV$	Hardness at time $t$
$H_0$	Initial hardness
$\Delta H$	Hardness drop
$k_1, k_2, k_3$	Constants in the ECCC hardness equation
$k_A$	Exponential constant for temperature dependence
$K, q$	Constants relating interparticle spacing to hardness
$K_S$	Fitting coefficient in the Masuyama hardness drop relationship
$LMP$	Larson-Miller parameter
$M, m$	Constants in Monkman-Grant relationship
$n$	Creep exponent in Norton's law
$p$	Correction constant in Allen-Fenton hardness model
$RL$	Replica level in [cavities/mm <sup>2</sup> ]
$S$	Dimensionless stress parameter

$t$	Time
$t_r$	Rupture time
$T$	Temperature
$u$	Scaling factor in the hardness relationship for straight pipes
$v$	Scaling factor in the hardness relationship for bends
$w$	Exponential factor in the hardness relationship for straight pipes
$z$	Exponential factor in the hardness relationship for pipe bends
$w_i, u_i, v_i, z_i$	Factors in the hardness relationships for straights and bends at a specific time $i$
$\alpha$	Exponential constant in the Failure Forecast method
$\alpha'$	Particle/dislocation interaction parameter
$\varepsilon$	Creep strain at time $t$
$\varepsilon_s$	Monkman-Grant constant
$\varepsilon_R$	Rupture strain
$\dot{\varepsilon}$	Strain rate
$\dot{\varepsilon}_0$	Initial/reference creep strain rate
$\dot{\varepsilon}_{min}$	Minimum creep strain rate
$\lambda$	Interparticle spacing
$\mu$	Shear modulus
$\sigma$	Hoop stress
$\sigma_0$	Orowan stress
$\omega$	Creep damage variable defined as cavity ratio
$\omega_{straight}$	Creep damage for straight pipes
$\omega_{bend}$	Creep damage for pipe bends
$\Lambda$	Secondary to tertiary creep strain ratio
$\Omega$	Creep damage variable in the Omega model

## 1. Introduction

Thermal power generation plants are under increasing pressure to maintain safe operation in a market that is challenging from both a revenue and regulatory perspective. Normal practice for the assessment of the condition of high temperature materials in-service is based on the acquisition and interpretation of data captured on outage for surface replica, hardness and strain which are, in general, utilized *individually* in various empirical models. These data are not easily, nor routinely, used in a predictive model for residual creep life assessment, with significant run-repair-replace decisions invariably based on very conservative assessments, advised by expert elicitation and intelligence gained from other similar assets in service.

There is great comfort in acquiring extensive field data during successive inspection campaigns, but the challenge is how to use this data efficiently to inform subsequent actions on plant [1]. Currently the overriding focus for health monitoring and assessment is placed on the data obtained from invasive inspections during an outage. Experimental studies on high temperature  $\frac{1}{2}\text{Cr}\frac{1}{2}\text{Mo}\frac{1}{4}\text{V}$  (CrMoV) materials retired from service has shown how this approach [2, 3] is very conservative. The currently-employed approach results in rapidly increasing inspection volume [1] as the plant ages and is only cost effective when the economics associated with plant operation are lucrative, which currently is not the case. During plant operation, limited assessments of creep rupture life are also made using operational steam temperature and pressure data, with well-established parametric relationships [4-6]. The challenge is how to better utilise and integrate this wide range of health monitoring data to reach more informed plant decisions.

In practical high temperature power plant health monitoring and life assessment, the role of hardness testing, surface replicas and strain measurement each play a part in the decision-making process that predicts the current condition of

the assets and influences subsequent outage scope. Moreover, the effectiveness of how and when to deploy these health monitoring and assessment techniques is influenced by the material type, age, operating history and to some extent the original fabrication process [7].

Hardness measurement is a standard non-destructive technique that, in combination with other methods, typically surface replication, is used to support life assessment decisions for high temperature creep. Hardness is defined as the material resistance to plastic deformation under an applied load on a given indenter type and is a function of material, temperature, ageing and stress. Precipitate coarsening and coalescence, decrease in dislocation density and recovery processes are among the main causes for a reduction in hardness in service, which eventually leads to creep cavity and crack formation and finally to an eventual failure of materials at high temperature [8]. For this reason, hardness is considered a practical measure that can be used to quantify material degradation in service [9].

The occurrence of creep cavitation is a precursor to creep crack initiation which leads to creep failure in ferritic steels. Hence a systematic approach for surface replica assessments on power plant materials is one of the key approaches used for practical life management. Surface creep replicas are typically targeted at locations that are assessed to be more likely to accumulate creep damage. The first parent material inspection would typically occur after ~ 50% of the assessed creep rupture life, with pipe bends being the highest priority location. The relevant inspection body will apply a set of assessment criteria [7] to the results of the surface replica, based on the cavitation count per mm<sup>2</sup> and on the degree of alignment or orientation of the observed creep damage at the grain boundaries. These assessment criteria are invariably based on some version of the semi-quantitative Neubauer [10] damage scale. This practical metallurgical assessment approach is used to support run-repair-replace decisions during an outage inspection and influences the scope of subsequent outage campaigns. It is important to note that current practice encourages taking surface hardness measurements at adjacent locations to creep replicas and is also complemented by material composition checks where necessary to confirm that design intent has been adhered to.

Strain assessment by measuring change in dimensions of targeted plant components is conducted periodically to predict the remnant creep life. Strain and strain rate are representative of material degradation [11], with high strain rates being exhibited as failure is approached.

For the first time, this paper explores trends obtained from an analysis of large datasets associated with plant inspection of parent CrMoV material. The capability, strength, and weakness of inspection methods (surface replicas, hardness and strain) currently deployed are explored and, on this basis, new empirical relationships are proposed that are informed from analysis of these plant datasets and reference to experimental testing. Models are developed based on data acquired from main steam straight and bend sections operating at ~ 173.8 bar and 568°C and a case study illustrates how the methods would be applied in a practical context for straight pipe sections.

Assessing the condition of the parent material on ageing plant is an additional challenge to that presented by the assessment of weld integrity. Inspecting, repairing, or replacing welds as they age can be reasonably managed and quantified, whereas decisions on the integrity of the extensive volume of parent material typically results in part or wholesale system renewal. Hence, more effective health monitoring and assessment of residual life has significant benefits as plant ages and decisions are required regarding whether to pursue major refurbishments.

## **2. Applications of Hardness, Replica and Strain Monitoring for Life Assessment**

### **2.1 Strain Life Models**

In 1982, Cane introduced a model for low alloy ferritic steels based on strain measurements rather than the application of traditional life fraction rules with the aim to overcome the conservativeness of creep design codes and allow for a more accurate life estimation [12]. Cane's model is developed from the original work of Kachanov and Rabotnov on

creep damage in order to relate the strain accumulated with the remaining fraction life neglecting the primary creep strain [13]. In the uniaxial case, the model takes the form of eq. (1):

$$\varepsilon = \varepsilon_R \left[ 1 - \left( 1 - t/t_r \right)^{\varepsilon_S/\varepsilon_R} \right] \quad (1)$$

The life fraction consumed is obtained from rearranging eq. (1):

$$t/t_r = 1 - \left( 1 - \varepsilon/\varepsilon_R \right)^{\varepsilon_R/\varepsilon_S} \quad (2)$$

where  $\varepsilon$  is accumulated total strain at any time,  $\varepsilon_R$  is the creep rupture strain,  $\varepsilon_S$  is the Monkman-Grant constant that represents the secondary creep strain,  $t$  is the creep time,  $t_r$  is the creep rupture time. The model is relatively insensitive to  $\varepsilon_R$  so that  $\varepsilon_S$  represents the only material parameter needed to assess residual life. Under low stress conditions,  $\varepsilon_S$  remains approximately constant in many materials [12]. Eq. (2) is of limited practical use for operational plant because the measure of accumulated creep strain can be inaccurate and is often unavailable. For this reason, the strain rate  $\dot{\varepsilon}$  is used rather than the absolute strain for remnant creep life calculation according to eq. (3) [11]:

$$\dot{\varepsilon} t = \varepsilon_S \left( t/t_r \right) \left( 1 - t/t_r \right)^{\varepsilon_S/\varepsilon_R - 1} \quad (3)$$

Cane's model was adopted within the former UK Central Electricity Generating Board (CEGB) [11] with modifications to allow non-uniform states of stress and temperature to be considered.

The concept of strain rate as a direct measure of material damage is also the underlying principle in the Omega method developed by Prager [14]. The constitutive equation of the model that describes the post-primary creep rate is expressed by:

$$\ln \dot{\varepsilon} = \ln \dot{\varepsilon}_0 + \varepsilon \Omega \quad (4)$$

where  $\dot{\varepsilon}_0$  is the initial or reference creep strain rate,  $\Omega = d \ln \dot{\varepsilon} / d\varepsilon$  is the creep strain rate acceleration factor which is a function of stress and temperature and defines the creep damage, and  $\dot{\varepsilon}$  is the instantaneous creep strain rate at time  $t$  [14]. The creep remaining life and the rupture life are estimated respectively through eqs. (5a) and (5b):

$$t_r - t = \frac{1}{\Omega \dot{\varepsilon}} \quad (5a)$$

$$t_r = \frac{1}{\Omega \dot{\varepsilon}_0} \quad (5b)$$

There is a striking similarity between eq. (5b) and the Monkman-Grant relation given in eq. (6) and the approximation of  $\dot{\varepsilon}_0$  to the minimum creep strain rate is often made [14].

$$t_r \dot{\varepsilon}_{min}^m = M \quad (6)$$

where  $M$  and  $m$  are material constants and  $\dot{\varepsilon}_{min}$  is the minimum creep strain rate.  $m$  generally varies in the range 0.8 – 1 while  $M$  has a broader range of variation depending on the alloy being considered [15].

The Cane, Omega and Monkman-Grant models can be essentially harmonised by the Failure Forecast method. This is a more recent empirical approach that predicts the remnant creep life based on the rate of change of a damage quantity and without the prior knowledge of stress state, temperature and material properties. The increase in the rate of change happens close to a criticality.

The application of the Failure Forecast framework to creep life assessment is a consequence of creep being a positive feedback damage mechanism where an increase in strain leads to an increase in strain rate after the minimum strain rate has been reached [16]. The remnant creep life is predicted with the Failure Forecast method by using eq. (7).

$$t_r - t = \frac{1}{A_0(\alpha - 1)} \left( \frac{1}{\dot{\varepsilon}} \right)^{\alpha-1} \quad (7)$$

where  $A_0$  and  $\alpha$  are best-fitting parameters that define the shape of the inverse rate-time curve and the gradient respectively. The projection of the best-fitting line through the inverse rate values allows the estimation of the failure time and is specific to a set of operating conditions. When  $\alpha = 2$  and the strain rate is substituted with the minimum strain rate, eq. (7) becomes the Monkman-Grant relationship. Also, the Omega method collapses to the Failure Forecast method assuming  $\alpha = 2$  and  $A_0 = \Omega$  even if  $A_0$  is not defined as a function of stress and temperature.

Application of a validated Failure Forecast approach is attractive to the plant operator because it utilises the rate of change of a monitored parameter, which is usually the focus of a plant operator when scrutinising inspection or health monitor data. Materials in high temperature applications invariably show a change in the rate of deterioration as they approach failure.

## 2.2 Hardness Models

Methods to evaluate the remaining life based on hardness measurements have been available for many years. The first significant contribution was given by Cane in 1985 [17] that formulated a hardness evolution law for low alloy ferritic steels by using the correlation between hardness and interparticle spacing. Cane's model has no practical plant application due to its complexity and difficulties in determining some key parameters such as hardness in solid solution and in the overaged condition [1]. Since hardness is a function of temperature and stress, relationships with the Larson-Miller parameter (LMP) to find the remaining life have been proposed. From the initial work of Gooch et al. on 1CrMoV rotor steel, the European Creep Collaborative Community (ECCC) developed a more general equation for low alloy ferritic steels shown in eq. (8) [18]:

$$\frac{HV(t, T)}{H_0} = k_1 LMP + k_2 LMP^2 + k_3 \quad (8)$$

where  $HV$  is the hardness measured at the time of inspection and  $H_0$  is the initial hardness before service that, if unavailable, could be found from a cold and unstress region of the same cast in the plant.  $k_1, k_2$  and  $k_3$  are non-dimensional material dependent fitting constants [18].

Cardoso, referring to the original work by Goto, introduced a modified function of hardness vs LMP to incorporate the effect of the applied stress in addition to thermal ageing. Under an applied load, the softening of the material is accelerated and consequently the hardness reduction is more evident [8].

In more recent years, Masuyama introduced eq. (9) to express the hardness drop as function of LMP for creep strength enhanced ferritic steels (P91, P92 and beyond) [9].

$$\ln(\Delta H) = K_s LMP \quad (9)$$

where  $K_s$  is a fitting coefficient related to the degree of applied stress [9]. Furthermore, Masuyama related the increase in creep strain  $\varepsilon$  with the increase in hardness drop  $\Delta H$  using eq. (10) [9, 19].

$$\ln(\Delta H) = A_1 \ln \varepsilon \quad (10)$$

where  $A_1$  is a fitting constant. Eq. (10) shows that the change in hardness drop can be used to estimate the creep strain and consequently the remaining life from the Omega method, the Monkman-Grant relationship or the Failure Forecast method [20]. Similarly, a novel empirical correlation between minimum creep strain rate and hardness was proposed by Morris et al. in [1] with the equation in the form:

$$\dot{\epsilon}_{min} = a \left( \frac{1}{HV} \right)^b \quad (11)$$

where  $a$  and  $b$  are fitting constants.

By using a multivariate analysis approach on Ni-based alloys, Saito et al. found a regression equation for hardness as a function of service temperature  $T$  and stress  $\sigma$  (eq. (12)) [20].

$$HV = 0.11252T + 0.075789\sigma + 36.86338 \frac{t}{t_r} + 95.33299 \quad (12)$$

Knowing the service temperature, the stress and the measured hardness, the creep life fraction  $t/t_r$  can be calculated from eq. (12) with an accuracy of  $\pm 18.5\%$  between the predicted and the measured hardness creep life fractions. The validation of the model requires the collection of much creep data under different test conditions and a process of parameter optimization to improve the prediction accuracy.

A similar approach based on multiple regression was followed by Allen and Fenton [21] to derive a creep rupture model for P91. The model is presented in eq. (13) and correlates the creep performances with the high temperature tensile properties in the same manner as in the Wilshire formulation [22]. Starting from an Arrhenius type function, Allen-Fenton use a normalised stress parameter,  $S/HV$ , where  $S$ =applied stress/flow stress, that characterises the high temperature properties of the material.

$$\ln t_r - \frac{Q}{RT} = \ln B - n \ln S + p \ln HV \quad (13)$$

where  $Q$  is the activation energy,  $R$  is the universal gas constant,  $B$  is a constant,  $T$  is the absolute temperature,  $n$  the Norton's law constant and  $p$  is a model correction constant [1]. The activation energy is assumed constant in the model while  $n$  and  $p$  are changing according to the applied stress. The limitation of the model is that the flow stress is not assumed temperature dependent resulting in an overprediction of creep life [1, 21].

### 2.3 Replica Models

There are many guides available describing how to take surface replicas and complete the creep cavity count assessment; it is worth noting that a high degree of expertise and experience is required to become competent on a particular material being examined.

More quantitative assessment methods have been proposed; those based on measuring the volume or area fraction occupied by cavities tend to be heavily influenced by the control of metallographic preparation, which makes these approaches difficult to use in a predictive life assessment model. Hence, researchers have tried to define mechanistic life models that use information from the metallurgy but are much less sensitive to the metallurgical preparation procedures. Examples of these models include those by Shamma [23] that define an 'A' parameter that is based on a fraction of the grain boundaries damaged by cavitation or cracking, which however still requires accurate detection of grain boundaries and damage.

$$\left( 1 - \frac{t}{t_r} \right) = (1 - A)^{nA/(A-1)} \quad (14)$$

where  $A$  is the ratio of secondary to tertiary creep strain. The relationship between the 'A' parameter and life fraction has been assessed for a range of 1CrMo and 2CrMo steels [24] however, the model appears to be too conservative compared to experimental data. Riedel [25] proposed a modification to the 'A' parameter model to reduce the excessive over conservatism and based on a more refined assessment of the damage occurring at the grain boundaries.

These quantitative models are not sufficiently refined to use in a practical plant assessment; however, the approaches where the metallurgical damage is ascribed to a life assessment model is interesting when considering more recent developments for assessing the level of creep damage using ultrasonic, electromagnetic [26] or alternating current potential drop (ACPD) [27] techniques. These are at various stages of development and (if successful in field applications) may provide the opportunity to develop more reliable quantitative life prediction models. The electromagnetic and ACPD techniques provide an assessment of the condition of the surface, or near surface region,

whereas the use of ultrasonic techniques has the potential to provide a volumetric assessment. The publication by Sposito et al [28] provides a useful overview of a wide range of non-destructive techniques used for the detection of creep damage in power plant steels.

Hence currently, the best quantitative surface replica life assessment model is based on a correlation of the Neubauer damage classification against life fraction, which has been reported by Shammas [23]. However, the correlations required by this approach are material specific and require calibration.

### 3. Service Exposure Observations for CrMoV

The service history of CrMoV main steam pipework parent material, originally installed in 1968 is investigated using hardness, replica and strain data collected during consecutive outages on three 500 MW coal-fired units identified with the acronyms Station A U1, U3 and Station B U3. Table 1 lists service hours and starts for which there is sufficient inspection data available on all three units, with the main steam system parent material operating at 173.8 bar and 568 °C conditions since first generation in 1968.

Table 1: Dates for available outages inspection records

	<b>Outage Year</b>	<b>Service Hours</b>	<b>Total Starts</b>
<b>Station A U1</b>	2005	221,799	2,740
	2009	242,536	3,552
<b>Station A U3</b>	2008	239,649	3,425
	2012	259,733	3,971
<b>Station B U3</b>	2008	239,335	2,178
	2012	262,348	2,492

For Station A U1, during the 2009 outage a diametral measurement survey was carried out on the main steam straight pipe sections at 100 feet level for two of the four main steam legs indicating negligible creep strain compared with historic data. High level of creep damage (high orientated/grouped creep cavities) were identified in several main steam pipe bends and straight pipes during the 2005 outage. Therefore, a strategic replacement of the highest risk areas was conducted during the 2009 outage. More precisely, 9 straight sections and 16 bends were proactively replaced, of which 6 straights and 4 bends had previously been reported to contain moderate-to-high levels of creep damage. Hardness measurements were recorded in 2009 for a total of 77 individual straight positions and 44 bend positions on the parent CrMoV main steam pipework.

For Station A U3, high levels of creep damage (high orientated/grouped creep cavities) were identified in several main steam bends and straights during the 2008 outage. Consequently, a strategic replacement programme of the highest risk area was carried out during the 2012 outage. In addition to the planned replacement, representative bends and straights were inspected in 2012. Aligned creep damage was recorded for some main steam pipework sections resulting in further unplanned replacements. A limited diametral survey was conducted in 2012 on main steam straight sections at the 100 feet level for one main steam leg and the results indicated minimal creep strain rates in accordance with historic data. Hardness measurements were also recorded in 2012 for a total of 204 straights positions against 72 in 2008 and 107 bends positions against 53 taken in 2008 on the parent CrMoV main steam pipework.

For Station B U3, planned strategic replacement was undertaken and additional replacements were required on the main steam pipework due to creep damage or defects during the 2012 outage. The microstructures of all bend and straight sections examined were typical of those expected for low alloy steel after long exposure at high temperatures, with some coarsening of both the inter and intra-granular carbides being evident. During the 2012 outage, hardness measurements were recorded on a total of 486 individual pipe positions, including 73 bends (against 46 bends inspected in 2008), providing sufficient data for meaningful statistical analysis. Across the tested CrMoV systems, hardness values varied between 111 HV and 225 HV. The mean value for bends was 134 HV and the mean value for straights was 138 HV, which is similar to the other units and representative of CrMoV on other similar stations. This overall mean hardness values show a significant reduction in hardness when compared with an average start-of-life value of ~170 HV.

## 4. The Relationships between Hardness, Replica and Strain

The focus of this investigation is on both pipe bend and pipe straight parent material with the worst condition expected for the bends since they represent a more critical location in the pipe system due to the effect of system loading, local thinning along the bend extrados and thickening along the bend intrados that occurs during fabrication [29, 30]. Two representative time-sets have been defined for the data assessment, with a time interval between these two time-sets of ~ 20 khrs, which represents a typical 4-year operating period.

- Time-set 1; based on outages occurring at 239,335, 239,649 and 242,536 hours. This comprises 209 hardness and surface replica data points.
- Time-set 2; based on outages occurring at 259,733 and 262,348 hours. This comprises 363 hardness and surface replica data points.

### 4.1 Investigation on Field Hardness and Replica Data

The hardness frequency distribution and the respective normal distribution for pipe straights and bends in time-set 1 and time-set 2 is plotted in Figure 1 and in Figure 2 respectively.

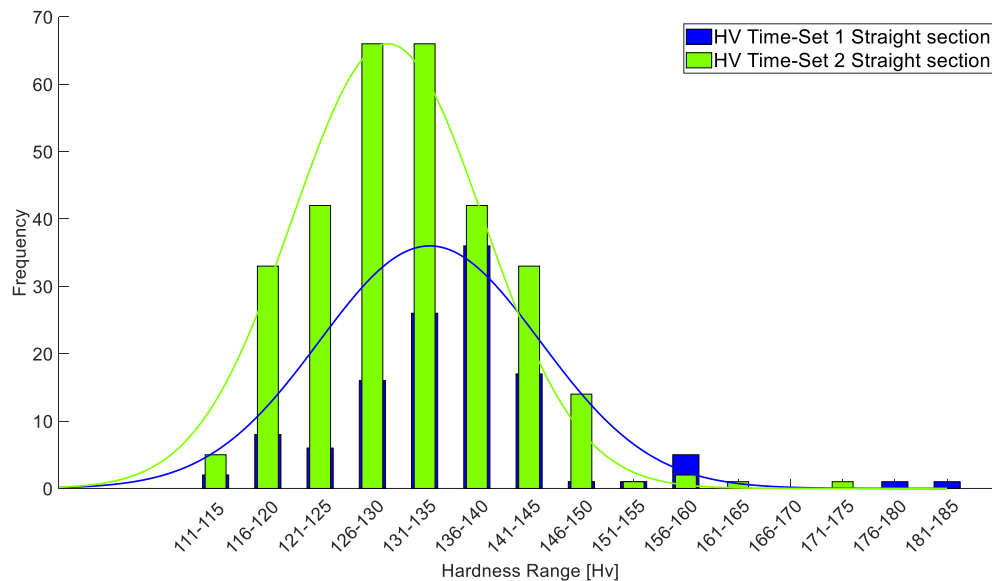


Figure 1: Hardness variation over two time-sets for CrMoV main steam straight pipes

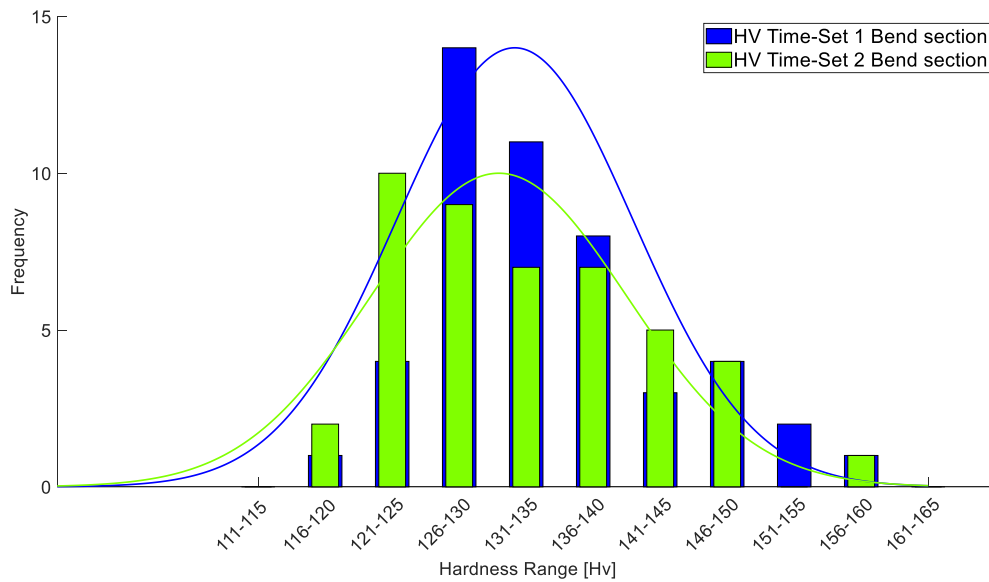


Figure 2: Hardness variation over two time-sets for CrMoV main steam pipe bends

Figure 1 shows a change in the straight pipe section population hardness, with the average value of 135.5 HV in time-set 1, reducing to 131.5 HV in time-set 2. Figure 2 shows a shift of the normalized curve as well indicating a decrease of hardness for the pipe bend sections. The average value is 134 HV in time-set 1, reducing to 132.9 HV in time-set 2.

Similarly, the creep replica level measurements associated with the two time-sets have been collected for the main steam pipe bends and straight pipes and are shown in Figure 3 and in Figure 4. The creep replica level is assigned following the counting of the cavities found in one mm<sup>2</sup> of the material microstructure according to the classification in Table 2.

Table 2: Terminology used to describe creep cavitation levels

Creep Cavity Damage Level	Microstructure	Cavity Density [cavities/mm <sup>2</sup> ]	Representative Cavity Density [cavities/mm <sup>2</sup> ]
1	Clear	0	0
2	Very Isolated	1 - 10	5
3	Isolated	10 - 50	50
4	Low Orientated	50 - 250	150
5	Mid Orientated	250	250
6	High Orientated	250 - 500	350
7	Grouped	500 - 1000	750
8	Aligned	1000 - 1500	1500
9	Microcracking	> 1500	> 1500

Figure 3 and Figure 4 do not seem to show a clear deterioration of the material microstructure between the two time periods. The replica level for time-set 2 is not clearly shifted in the right direction towards higher cavitation levels according to the replica classification (Table 2). This is possibly because as reported in the inspection reports, the pipe straights and bends found with 'high orientated', 'grouped', 'aligned' and 'micro-cracking' cavities in time-set 1 have been replaced directly during the same outage, thereby removing occurrences of the more damaged pipe sections from the population. In addition, the increase in the number of inspections (frequency) identifying 'clear' and 'very isolated' replica classifications in time-set 2 is attributed to plant ageing that has prompted an increase in the volume

of inspections. Considering the CrMoV material, service experience shows that once cavitation is detected in parent material at the ‘very isolated’ level 2 it takes ~ 2 operating cycles (40 khr) before damage levels 5-7 is reached, hence prompting removal from service.

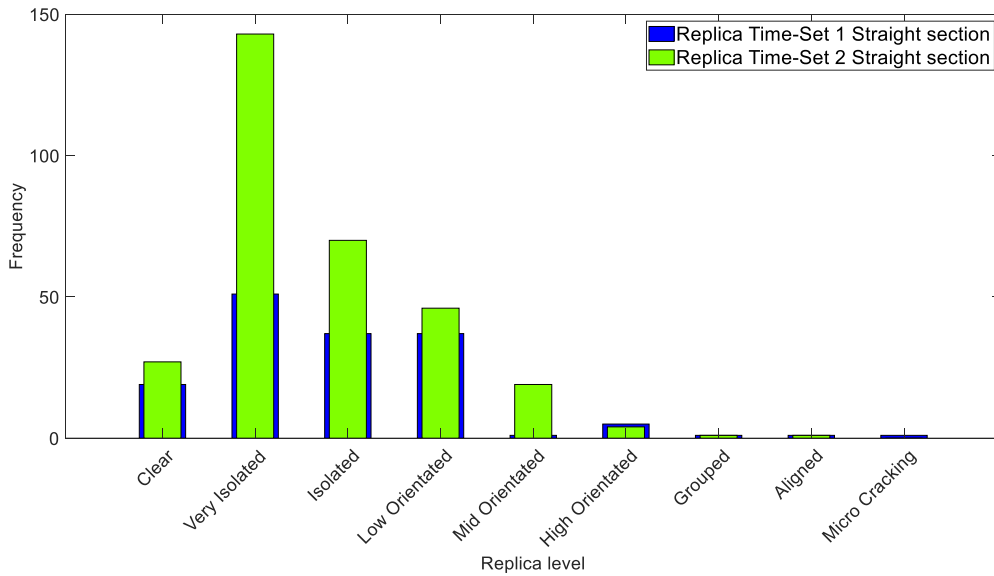


Figure 3: Replica variation over two time-sets for CrMoV main steam straight pipes

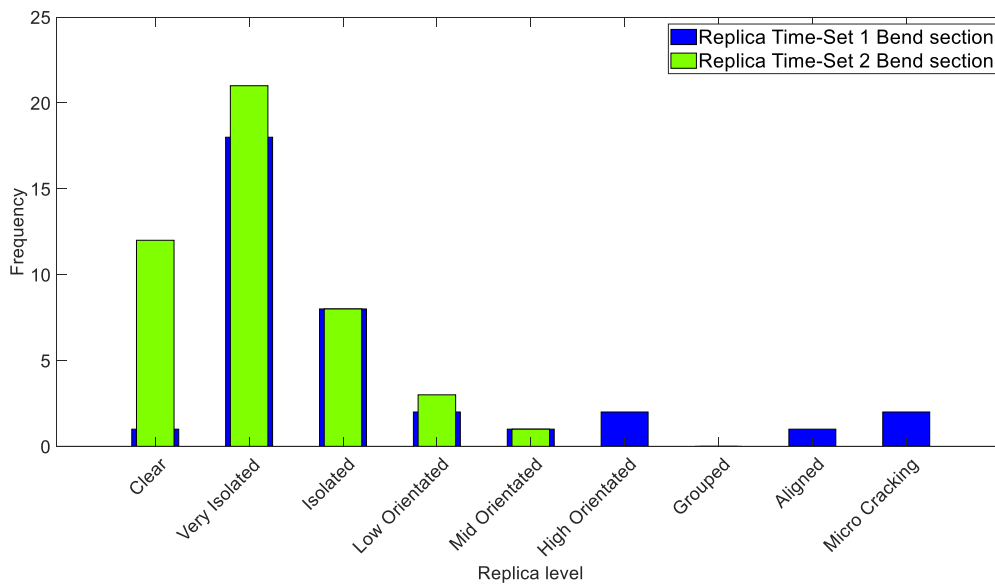


Figure 4: Replica variation over two time-sets for CrMoV main steam pipe bends

This illustrates the difficulty in interpretation of surface replication results with respect to residual life attributed to material in-service. The key indicator showing a change in the material microstructure and condition is observed in the shift in the population statistics highlighted in the hardness graphs, Figure 1 and Figure 2.

Another pipe specimen from the same original population was removed after ~ 272 khr of service, a slightly longer time in service than time-set 2 [3]. Four tensile specimens were extracted from different positions through the 60 mm pipe wall and tested at a service temperature of 570°C, with an average 0.2% yield strength of 170 MPa and tensile

strength of 207 MPa. These compared to original cast values of 220 MPa and 340 MPa respectively at 570 °C. This 23% reduction in yield strength and a 40% reduction in tensile strength is a significant reduction in strength. There was little difference recorded in the specimen yield and tensile strength values through the pipe thickness. In addition, the through section hardness range was 130-136.5 HV, taken in the radial direction, with a similar hardness range taken from the four specimens in the hoop direction. These values are consistent with data in the two time-sets. This highlights the potential for hardness data acquisition to be used in life assessment since the time span available to detect a change is much greater than for surface replicas.

## 4.2 Proposal for Empirical Relationships for Hardness and Surface Replica

For each time-set population the hardness data associated with a specific replica assessment level has been collated into population samples for straights and bends.

### 4.2.1 Hardness and Replica for Straight Pipes

The hardness mean and the standard deviation for each replica-hardness sample have been computed for time-set 1 and time-set 2 as shown in Figure 5.

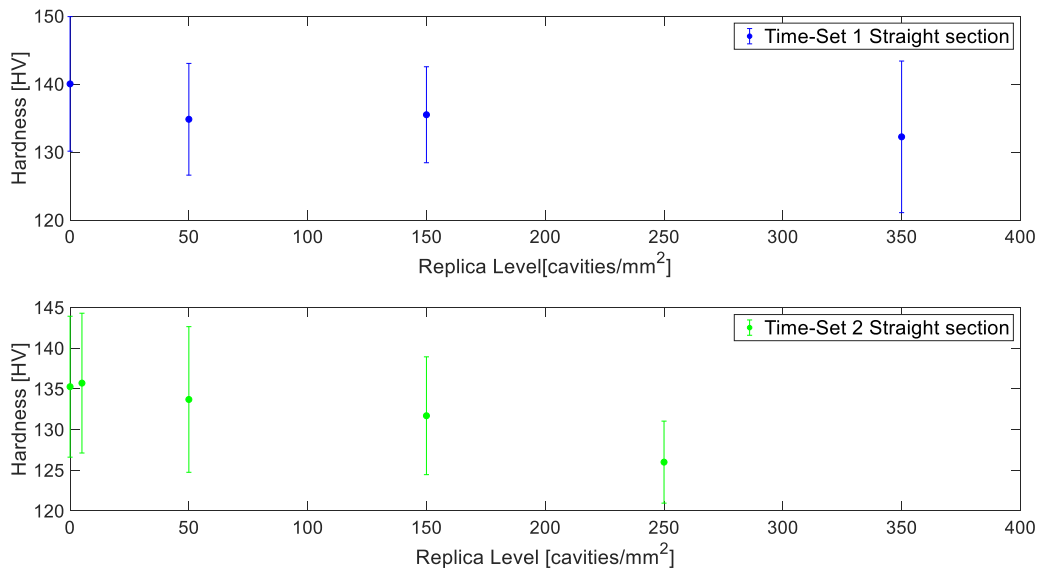


Figure 5: Hardness mean with standard deviation over two time-sets as function of cavities count for CrMoV straight pipes

The highest standard deviation value for time-set 1 is for the ‘high orientated’ replica level (350 cavities/mm<sup>2</sup>), equal to 11.4 HV, while for time-set 2 is equal to 9 HV for the ‘isolated’ replica level and similar to the ‘clear’ and ‘very isolated’ replica classes. A maximum sample variation of 11.4 HV can be expected from a field survey; however, this is too small to show appreciable changes in the microstructure. The standard error of the population has a maximum value of 5.5 HV.

The relationship between hardness and replica level has been determined using bespoke MATLAB coding based on hardness mean values from Figure 5 to give the lowest sum of squares error (SSE) value and the highest R<sup>2</sup>. The optimal relationship found for straight sections for time-set 1 and time-set 2 is shown in Figure 6.

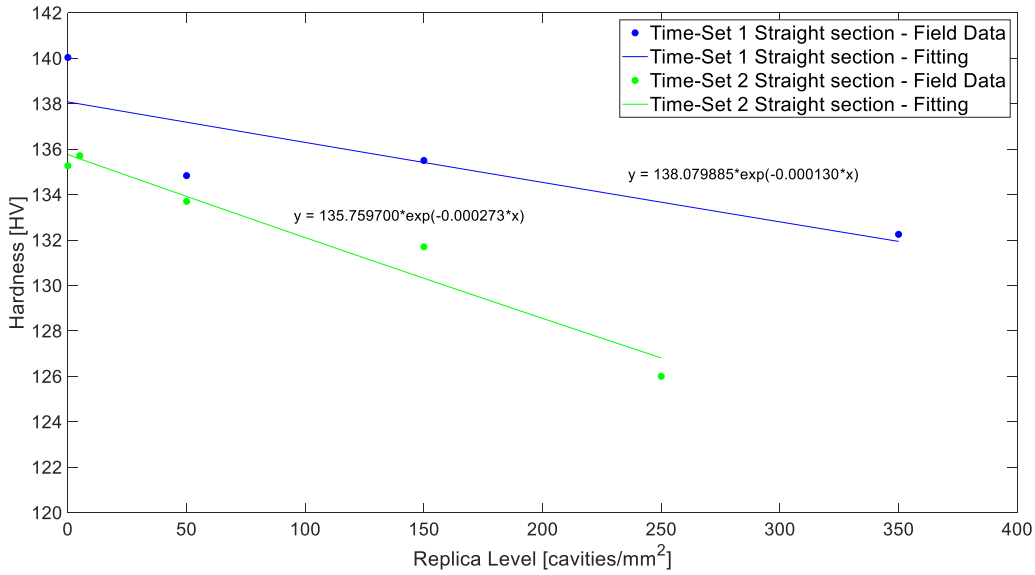


Figure 6: Hardness and creep damage (replica) relationship over two time-sets for CrMoV straight pipes

The best fit for main steam pipe straights hardness-replica field data is represented for the two time-sets by an exponential function with one term. The exponential functions are reported for clarity in Figure 6. The goodness of fit improves from time-set 1 to time-set 2 (SSE=2.8 and  $R^2=0.95$ ) where more field data is available to perform fitting considerations.

The general form of the function is given in eq. (15):

$$HV = u(t) \exp^{w(t) RL} \quad (15)$$

where  $HV$  is the hardness measured in [HV],  $RL$  refers to the creep damage in [cavities/mm<sup>2</sup>] measured with the replica technique,  $u$  and  $w$  are two fitting parameters and a function of time  $t$  in [hours].

- $w$  is a coefficient with unit of measure [cavities/mm<sup>2</sup>]<sup>-1</sup> that describes the decay rate of the function, has negative values and is greater with increasing service time.
- $u$  is a scaling factor that multiplies the whole function and is related to the hardness with the same unit of measure [HV]. When there are no cavities,  $u$  assumes the value of hardness for a specific time meaning it is indicative of the hardness decay of the material due to thermal ageing effects on the microstructure. When cavitation is present, the real value of hardness at time  $t$  is acquired when  $u$  is multiplied with the contribution given by cavities through the replica measure.

The values of  $u$  and  $w$  at time-set 1 and time-set 2 are reported in Table 3.

Table 3: Fitting parameters values for eq. (15) for straight pipe sections

		<b>Time-Set 1</b>	<b>Time-Set 2</b>
Straight Pipes	$u$	138.08	135.76
	$w$	-0.000130	-0.000273

The time dependency of  $u$  and  $w$  is extracted using the linear functions in eqs. (16) and (17) which have been obtained fitting the known values of  $u$  and  $w$  for the considered time-sets.

$$u(t) = -1.2315e^{-04}t + 167.85 \quad (16)$$

$$w(t) = -7.58e^{-09}t + 0.0017 \quad (17)$$

From eqs. (16) and (17) some observations can be made. At service time 0, which is the year of installation 1968, the value of coefficient  $u$  is 167.85 which corresponds to the received material Vickers hardness through eq. (15) when no cavitation is present. According to BS EN 10222-2 Table 1 [31], the room temperature tensile strength range for CrMoV (14MoV6-3) is 460-610 MPa depending on the manufactured supply. Using the relationship between hardness and tensile strength given in [32], the corresponding hardness range is 149-190 HV. The initial hardness value calculated with eqs. (15) and (16) for CrMoV straight sections can be therefore considered a good approximation of the start of life hardness for CrMoV.

Coefficient  $w$  assumes positive values until 224,590 service hours which, following eq. (15), implies an increase of hardness. These values are neglected because they give an incorrect interpretation of the processes involved in the change of the microstructure. Up to 224,590 service hours, the hardness change in straight sections is not influenced by creep cavitation but by thermal ageing effects that cause the softening of the material. After 224,590 hours, creep damage caused by cavities causes an acceleration in the reduction of hardness for straight sections of CrMoV operating at 173.8 bar and 568 °C conditions.

Combining eqs. (15) with eqs. (16) and (17), eq. (18) is obtained:

$$HV = (-1.2315e^{-04}t + 167.85)exp^{(-7.58e^{-09}t+0.0017)RL} \quad (18)$$

Eq. (18) is a more general equation that combines 3 main variables, i.e. time, hardness, and replica count and can therefore be considered a master equation for CrMoV parent material straight pipe sections. Inserting the time in [hours] and the replica level in [cavities/mm<sup>2</sup>], the hardness value is evaluated or vice versa, knowing the hardness from field inspection the corresponding value of replica is obtained. Therefore, eq. (18) allows projections over time of hardness or replica as has been extrapolated in Figure 8 for hardness.

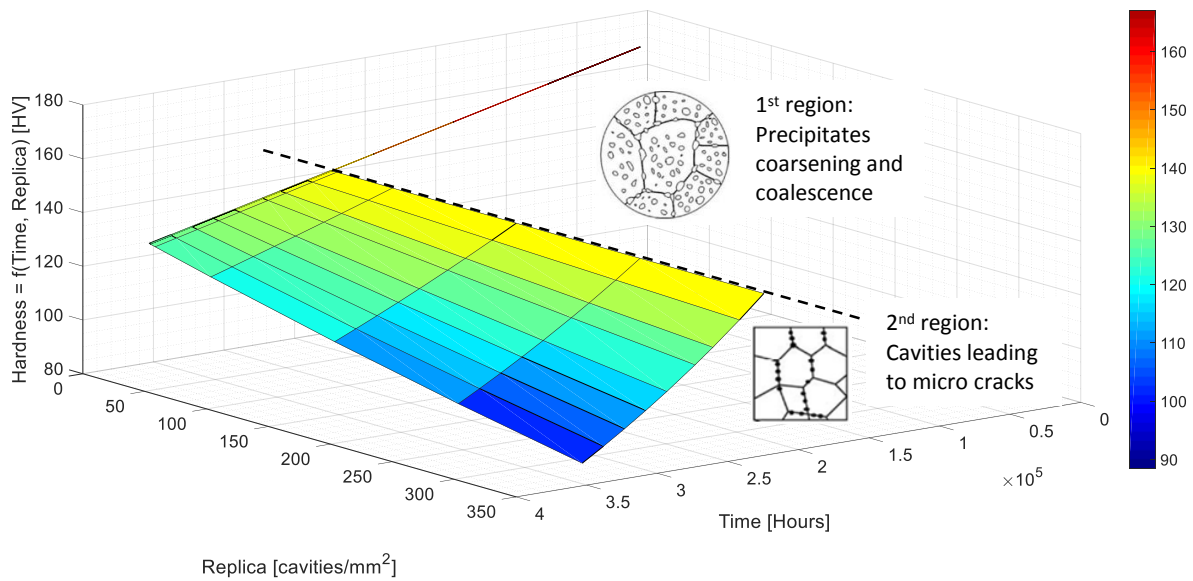


Figure 7: Hardness projection over replica for a selected time range for CrMoV straight pipes

Two regions can be distinguished from Figure 7. The first, associated on the graph with ‘Clear Replica Level’, from the installation year to 224,590 hours, in which the hardness variation is not dependent upon creep cavities. As mentioned before, the hardness variation in this region is attributed to softening processes that happen over the time due to temperature exposure. The second region, from 224,590 hours, where the effect of creep cavities on hardness reduction is more significant and combines with thermal softening.

#### 4.2.2 Hardness and Replica for Pipe Bends

The same approach used for straights has been followed for the analysis of pipe bends. Figure 8 shows the average value of hardness and its standard deviation for corresponding replica levels.

In the data selection process, replica levels associated with three or less hardness counts have been discarded because of insufficient data to give a reliable average hardness value.

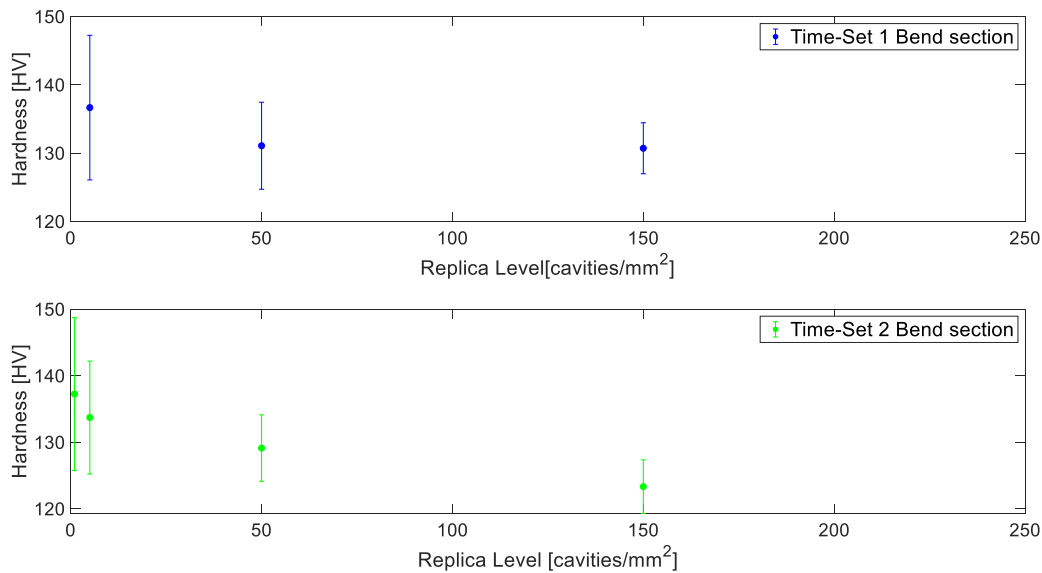


Figure 8: Hardness mean with standard deviation over two time-sets as function of cavities count for CrMoV pipe bends

In Figure 8, the maximum standard deviation for time-set 1 is found for ‘very isolated’ creep replica and is equal to 10.6HV while for time-set 2 is found for ‘clear’ creep replica and equal to 11.5HV. These results are in accordance with the findings for time-set 2 in Figure 5 where the maximum standard deviation is associated with ‘very isolated’ or ‘isolated’ replica levels but close to the value for ‘clear’ replica level. The higher variability of hardness data seen for lower replica classes suggest a greater difficulty in distinguishing between ‘clear’, ‘very isolated’ and ‘isolated’ classes during the cavities count process.

The fitted relationships for CrMoV parent bend sections for time-set 1 and time-set 2 is shown in Figure 9.

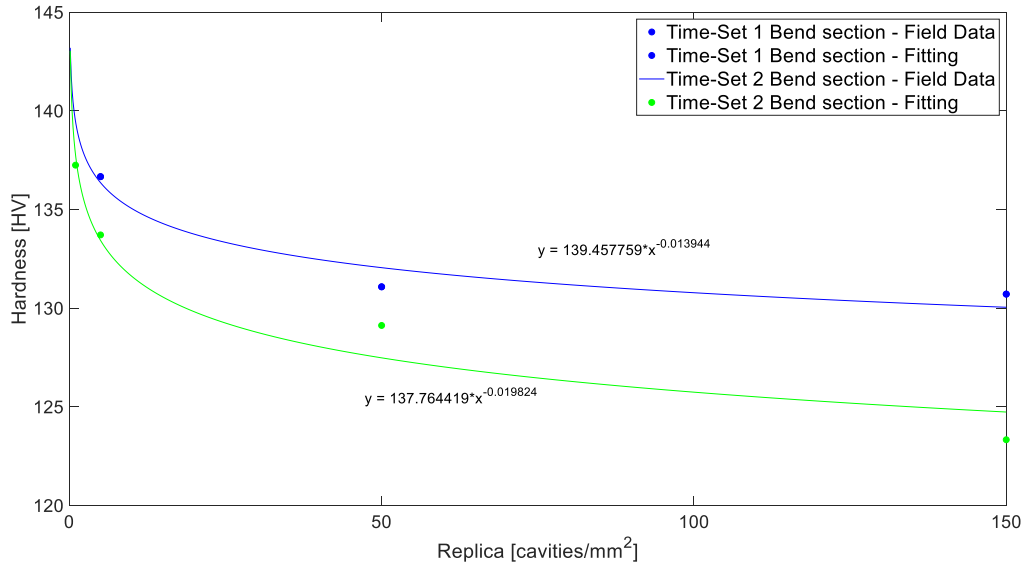


Figure 9: Hardness and creep damage (replica) relationship over two time-sets for CrMoV pipe bend

As shown in Figure 9, the best fitting for pipe bends is represented by a power function with a goodness of fit for time-set 1 of SSE=1.48 and  $R^2=0.933$  and for time-set 2 of SSE=5 and  $R^2=0.95$ .

The general form of the power equation is:

$$HV = v(t)(RL)^{z(t)} \quad (19)$$

where  $HV$  is the hardness measured in [HV],  $RL$  refers to the creep damage measured in [cavities/mm<sup>2</sup>],  $v$  and  $z$  are two fitting parameters function of time  $t$ .  $v$  and  $z$  have the same meaning as  $u$  and  $w$  for pipe straights.  $z$  defines the decay of the power function and has units of [cavities/mm<sup>2</sup>]<sup>-1</sup> while  $v$  is the scaling factor that assumes the unit of measure of hardness [HV] to relate creep damage and hardness. The variation of  $v$  and  $z$  over time are reported in Table 4.

Table 4: Fitting parameters values for eq. (19) for pipe bend sections

		Time-Set 1	Time-Set 2
Pipe Bends	$v$	139.46	137.76
	$z$	-0.0139	-0.0198

The linear functions that describe the variation of  $v$  and  $z$  over time are presented in eqs. (20) and (21):

$$v(t) = -8.98e^{-05}t + 161.2 \quad (20)$$

$$z(t) = -3.12e^{-07}t + 0.0615 \quad (21)$$

From eq. (20) at service time 0 (year of installation 1968),  $v = 161.2$  that gives an initial value of hardness for bends of 161.2 HV using eq. (19) when no cavities are detected. The value of 161.2 HV is within the hardness range of 149-190 HV calculated from reference [32]. The difference with the initial hardness for straights can be due to a different manufactured supply, hence the importance of tracking the change in hardness through life and when replicas start to show cavities. Another reason can be attributed to the manufacturing process that causes the bend to be a weak point in the pipe system [33]. Coefficient  $z(t)$  is positive up to 197,060 hours that implies an incorrect increase in hardness

from eq. (19). These values are therefore discarded and only negative  $z(t)$  values are considered for the correct estimation of hardness-replica relationship. Before 197,060 hours, eq. (19) is not valid in describing creep cavitation because the hardness change is mostly influenced by microstructural softening processes as it has been discussed in section 4.2.1 for the straights and later in section 4.2.3.

It is important to underline that the effect of creep cavities damage on bends starts after 197,060 hours while for straights the hardness change due to creep cavities starts later from 224,590 hours. This is mainly attributed to higher stresses acting on the bends. The main steam system design pressure is 173.8 bar with an outer diameter of 342 mm and 60 mm thickness for straight sections. The calculated mean diameter hoop stress for straights is 40.8 MPa. The pipe bends are characterized by a variation in thickness with a minimum in the bend extrados due to the manufacturing processes. Among different analysed bends measured in different positions, it has been reported an average thickness of 57.8 mm in the extrados. Discounting the effects of pipe system stress, the pressure induced hoop stress in bend is equal to 42.4 MPa, based on the extrados wall thickness, compared to the lower hoop stress in the straights. This enhanced stress will contribute to a faster deterioration rate in bends.

The general function for pipe bends obtained from combining eqs. (19), (20) and (21) is expressed in eq. (22).

$$HV = (-8.98e^{-05}t + 161.2)(RL)^{(-3.12e^{-07}t+0.0615)} \quad (22)$$

Eq. (22) is the master equation for CrMoV pipe bend parent material that relates time in [hours], hardness in [HV] and replica count in [cavities/mm<sup>2</sup>].

Figure 10 shows the hardness projection over time and creep replica level calculated from eq. (22).

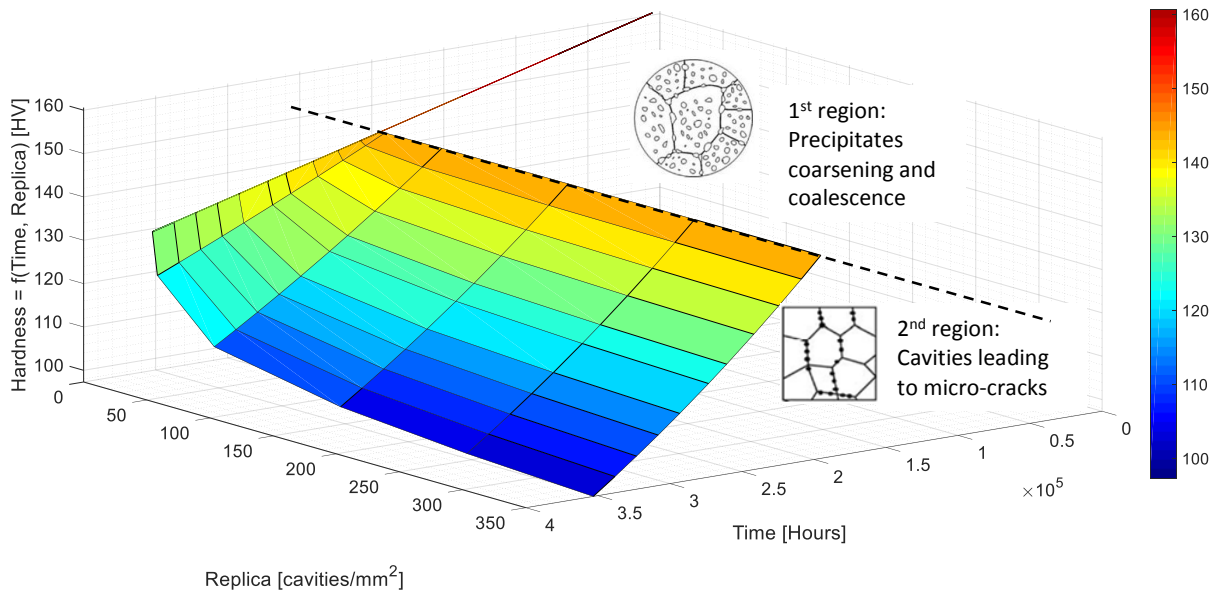


Figure 10: Hardness projection over replica for a selected time range for CrMoV pipe bends

As for the straight sections in Figure 7, also in Figure 10 there are two distinguished regions in the creep behaviour of pipe bends. In the first region until 197,060 service hours the creep behaviour is dominated by the effect of precipitates coarsening and their coalescence that lead to the second region where cavities nucleate up to the formation of micro-cracks.

### 4.2.3 Creep Strain and Damage Assessment as Function of Hardness and Replica

The correct prediction of creep strain, and consequently of remaining creep life, is determined by the combination of different microstructural processes. Precipitates coarsening and creep cavitation have been identified as the two main conditions leading to creep damage in low alloy steels such as CrMoV [17].

During service exposure, thermal ageing is responsible for the evolution, coarsening and agglomeration of carbides and in combination with the primary stress arising from system operating pressure and other sources such as pipe system loading, for the subsequent nucleation of creep cavities. New secondary carbides species, mostly  $M_{23}C_6$ ,  $M_6C$ ,  $M_2C$  and  $M_7C_3$  in CrMoV steels depending on process conditions and chemical composition [18, 34, 35], precipitate mainly along the material grain boundaries due to the transfer of Cr and Mo from the metal matrix to the carbides (Figure 11(a)). The depletion of strengthening elements in the metal matrix and the change of carbide structure cause a reduction in the mechanical resistance of the material in terms of yield strength, creep rupture strength and in the material hardness [15]. The subsequent agglomeration of carbides, due to the extended exposure to operation conditions, reduces the quantity of finely distributed carbides in the metal matrix and by facilitating the movement of dislocations, triggers cavity formation (Figure 11(b)) causing a further softening of the material mechanical properties [18]. The nucleation of cavities from carbides at grain boundaries is recognized to be the most probable nucleation mechanism [36, 37].

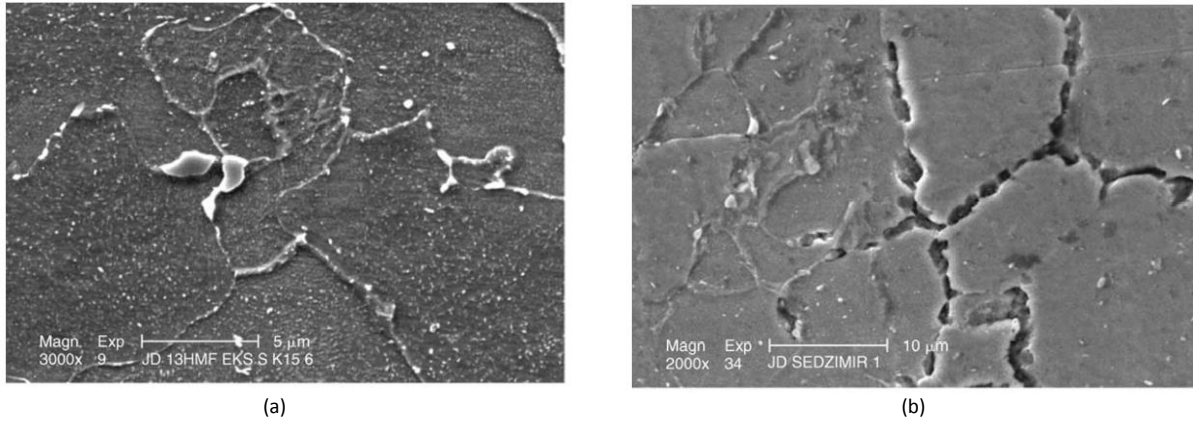


Figure 11: (a) SEM micrograph showing carbides coalescence visible along CrMoV grain boundaries [35], and (b) SEM micrograph showing orientated cavities along CrMoV grain boundaries [35]

These two dominant mechanisms, carbide precipitation and creep cavitation, have been also identified in Figure 7 and in

Figure 10 where the two regions of hardness change are related respectively to precipitates softening and creep cavitation. While in the first region, softening caused by precipitate coarsening is considered the predominant damage condition, in the second region, the two processes occur simultaneously but cavitation plays the most relevant role in leading to failure. Therefore, in the following paragraph, two methods, which reflect this change in material behaviour, are developed to model creep strain as function of surface hardness and replica condition.

The first method aims to describe the impact of hardness decrease due to particle coarsening on the material creep strain rate when no or insufficient cavities are detected from a surface replica. By expressing the dependence of stress and temperature to the minimum creep rate with the Norton's power law and an Arrhenius type law, eq. (23) is formulated:

$$\dot{\epsilon}_{min} = A_2 \exp(k_A T) \left( \frac{\sigma}{\sigma_0} \right)^n \quad (23)$$

where  $A_2$  and  $n$  are respectively the creep coefficient and the creep exponent according to Norton's law that vary according to the stress/temperature regime [38].  $k_A$  is an exponential constant with unit  $[1/K]$  expressing the

dependence with temperature and  $T$  is the absolute temperature in Kelvin [39].  $\sigma_o$  is the Orowan stress and as described by Cane [17] and by Dyson [39] and is the critical stress value required to move the dislocations past the particles obstacles characterizing in this way the tendency for plastic flow of the metal [40]. In Allen-Fenton [21]  $\sigma_o$  is the flow stress taken as the average between the yield and the ultimate tensile strength but both are an expression of the plastic deformation of the material.  $\sigma_o$  is inversely proportional to the interparticle spacing  $\lambda$  (eq. (24)) that has been demonstrated to be correlated with the hardness (eq. (25)) [17].

$$\sigma_o = \frac{\alpha' \mu b_1}{\lambda} \quad (24)$$

$$\lambda = K/HV^q \quad (25)$$

where  $\alpha'$  is the particle/dislocation interaction parameter,  $\mu$  is the shear modulus in [GPa] and  $b_1$  is the Burgers vector in [nm] [17]. Substituting eqs. (24) and (25) in eq. (23), eq. (26) is obtained:

$$\dot{\epsilon}_{min} = A_2 \exp(k_A T) \left( \frac{K}{\alpha' \mu b_1} \right)^n \left( \frac{\sigma}{HV^q} \right)^n \quad (26)$$

And finally, the rupture time  $t_r$  is estimated recalling the Monkman-Grant relationship with the minimum creep strain rate:

$$t_r = B \exp(-k_A T) \left( \frac{\alpha' \mu b_1}{K} \right)^n \left( \frac{HV^q}{\sigma} \right)^n \quad (27)$$

Equation (27) is very similar to the final expression given by Allen-Fenton in eq. (13) [21] and by Morris et al. in eq. (11) [1] with the addition of stress dependence and the characteristic parameter  $(\alpha' \mu b_1)/K$  that is typical of the microstructure.

Creep cavitation is considered the dominant mechanism in the second region contributing more than just precipitation coarsening to the material loss of strength and consequently to the increase of creep strain rate as underlined in

Figure 7 and

Figure 10. Therefore, in the second method, the effect of creep cavitation on strain rate is investigated by considering the continuum creep damage mechanics (CDM) model introduced first by Kachanov-Robotnov. The Kachanov-Robotnov model is an empirically-based CDM model that herein is used for its simplicity in describing the relationship between the creep rate and the damage parameter with a power-law expression. Its inherent limitation occurs when the damage parameter approaches unity, which can be overcome by using more complex models such as the Liu-Murakami and the Dyson formulations [39, 41, 42] but the basic concepts will remain unchanged.

The Kachanov-Robotnov model [43-45] with the inclusion of the temperature dependence by an Arrhenius type law is as follows:

$$\dot{\epsilon} = A_2 \exp(k_A T) \left( \frac{\sigma}{1 - \omega} \frac{1}{\sigma_o} \right)^n \quad (28)$$

where  $\omega$  is the damage parameter, which effectively represents the area covered by microcracks and cavities and varies from 0, the undamaged state, to 1 at failure [46]. To account for the inspection data and the ability to represent material degradation, the damage parameter  $\omega$  in a real industrial application can be thought to be defined in accordance with eq. (29):

$$\omega = \frac{\text{cavities at time } i}{\text{max acceptable cavities}} = \frac{RL}{\text{cavities}_{max}} \quad (29)$$

The advantage of using eq. (29) to define the damage is its practicality. Cavities are counted directly from creep replication [cavities/mm<sup>2</sup>] allowing for the assignment of a creep damage level to the inspected component according to the criteria in Table 2. The maximum number of cavities  $cavities_{max}$  is represented by the highest acceptable damage level that triggers replacement actions, with  $RL$  representing the cavity density measured at time  $t$ . Observations show that this reference level typically corresponds to the ‘high orientated cavities’ level that according to Table 2 is 250 cavities/mm<sup>2</sup>. The new defined damage parameter  $\omega$  in eq. (29) always varies from 0, the undamaged state without cavities, to 1, the full damaged state.

Rearranging eq. (29) to include the relationship between creep replica and hardness for straight pipes and pipe bends according to eqs. (15) and (19) respectively, eqs. (30) and (31) are obtained:

$$\omega_{straight} = \frac{\frac{1}{w_i} \ln \frac{u_i}{HV_i}}{cavities_{max}} \quad (30)$$

$$\omega_{bend} = \frac{\left(\frac{v_i}{HV_i}\right)^{1/z_i}}{cavities_{max}} \quad (31)$$

where  $w_i, u_i, v_i, z_i$  are the coefficients in the hardness equations calculated at time  $i$ .

The advantage of eq. (28) combined with eqs. (30) and (31) and previously of eq. (23) is to allow a direct formulation of the creep rate as function of the main creep characteristic parameters, i.e. stress and temperature operating parameters and routinely collected hardness and replica that give an insight on the microstructure condition of the material.

Recalling the strong dependence of the rupture time to the secondary creep strain through the Monkman-Grant relationship and its insensitivity to the rupture strain as stated in [12], the rupture time in the second region is estimated as:

$$t_r = B \frac{(1 - \omega)^n \sigma_o^n}{exp(k_A T) \sigma^n} \quad (32)$$

Equation (32) can be reconnected to the rupture time expression given by the Omega method in eq. (5b) where the creep damage  $\Omega$  has been expressed by the  $\omega$  parameter defined through inspection data.

Equations (23) and (28) could be used as a proactive condition monitoring technique combined with on-site strain measurements for the estimation of the material remaining life by substituting the strain rate in the general expression for creep life in eq. (7).

### 4.3 The Role in Health Monitoring based Life Assessment

The new approach for health monitoring using routine monitoring data such as hardness, replica metallography and strain measurements is summarized in the flowchart in Figure 12.

A first estimate of rupture time can be obtained through the Failure Forecast Method in eq. (7) when sufficient strain measurements are available to allow the calculation of the strain rate. Another possible use of the Failure Forecast Method would be with the measure of hardness change through successive outages with sufficient data.

The hardness and replica cavities count relationship is applied according to the pipe component (bend or straight). This relationship is used to develop creep strain rate models and consequently it allows a prediction of rupture time. In this paper, eqs. (27) and (32) have been developed for CrMoV pipes to define the rupture time in the softening and in the cavitation regions, respectively, according to the material condition. Strain measurements could also be correlated with hardness and replica count data. The prediction of rupture time obtained from the different methodologies is then compared to check for convergence and thus confirm a value for rupture time or further review [15].

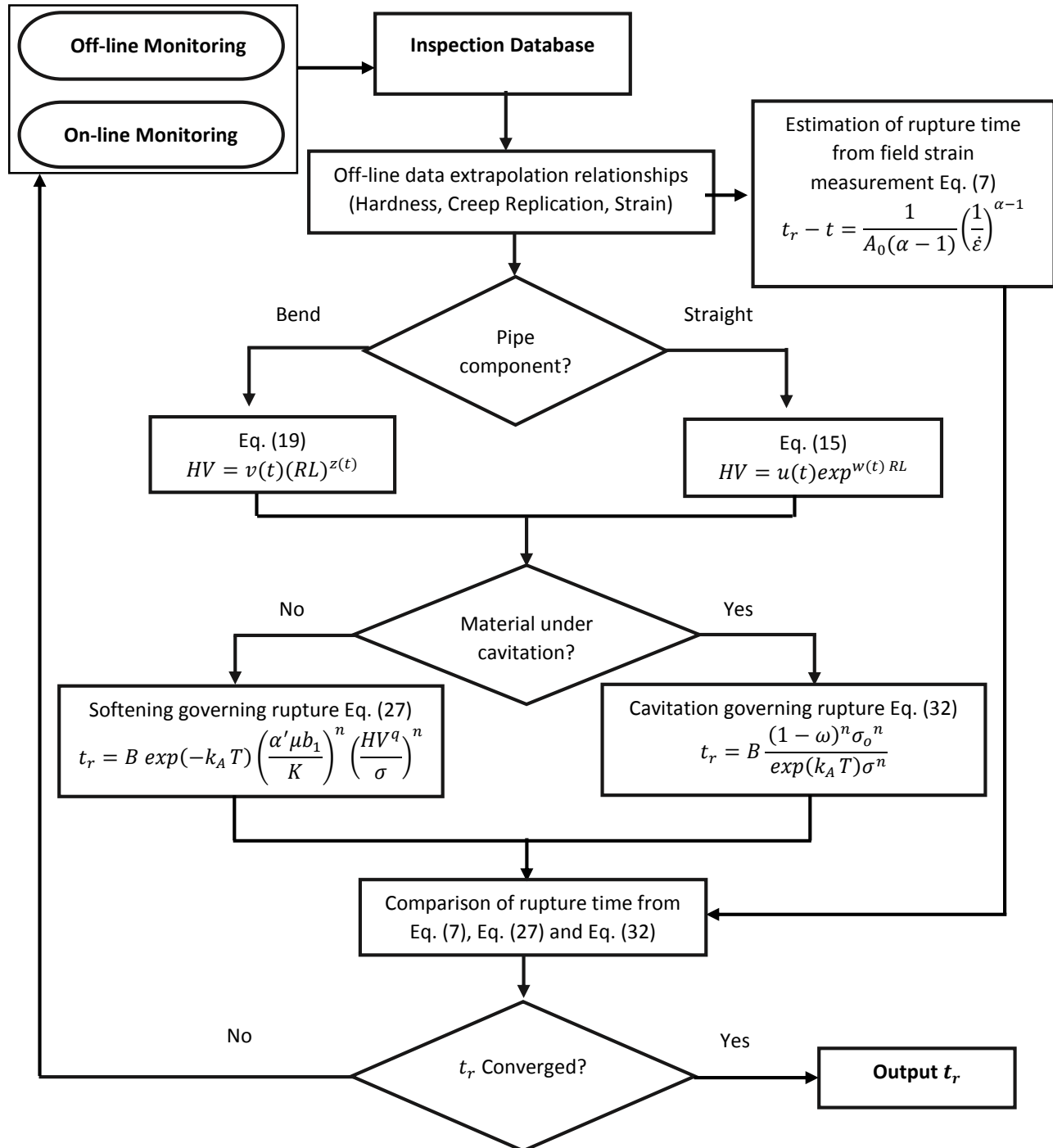


Figure 12: Flowchart of the health monitoring approach utilising site inspection data

## 4.4 Case Demonstration

The implementation of the flowchart in Figure 12 is approached in the following case demonstration where the rupture time is estimated using parameters available in literature and field data extracted from sections 4.2.1 and 4.2.2.

The example is referenced to a straight pipe section, but the same approach is applicable for bends. The creep strain rate and consequently the rupture time will be calculated for the particle coarsening and the creep cavitation regions following eqs. (26)-(28) and (32). The input parameters that are used in the equations are given in Table 5.

Table 5: Constants of creep strain rate model

$A_2$	$k_A$ [1/K]	$T$ [K]	$K$ [ $\mu\text{mHV}$ ]	$q$	$\alpha'$	$\mu$ [MPa]	$b_1$ [ $\mu\text{m}$ ]	$n$	$M$	$\sigma$ [MPa]	$B$
$4.2 \times 10^{-35}$	0.053	841.75	$3.34028 \times 10^{17}$	8.2133	0.228	63200	$2.45 \times 10^{-4}$	4	0.013	40.8	$8.59 \times 10^{28}$

The temperature  $T$  and hoop stress  $\sigma$  are typical operational power plant conditions and the value of the creep rate stress exponent  $n$  is typical for service conditions at low stress regime [47]. The constants  $A_2$ ,  $k_A$ ,  $\alpha$ ,  $\mu$  and  $b_1$  are taken from [17] as well as  $K$ ,  $q$  that are extrapolated from the interparticle spacing-hardness relationship.

$M$  is the Monkman-Grant constant taken from [15] and  $B$  is calculated from  $M$  and  $A_2$ . For the first region in which the precipitate coarsening is the principal degradation mechanism and the cavity number is negligible, the minimum creep strain rate is computed in units of  $\text{s}^{-1}$  with eq. (26) using hardness values obtained from eq. (18) with  $RL = 0$  at chosen different service times. The estimated creep life is computed from eq. (27).

In the second region where the rupture time is influenced mainly by creep cavitation, the same procedure is followed considering  $RL \neq 0$  with the number of cavities taken from field measurements. The strain rate is estimated using eq. (28) through  $\omega$  in eq. (30) for straight pipes and the remaining rupture time is given by eq. (32).

The results of creep strain rate together with the estimated creep life are shown in Table 6 in units of  $\text{hrs}^{-1}$  and hrs, respectively.

Table 6: Estimated hardness, strain rate and rupture time

Service Hours [khrs]	Cavity Density [cavities/ $\text{mm}^2$ ]	HV	$\omega$	Strain Rate [1/hrs]	$t_r$ [hrs]
0	0	168	0	$6.39 \times 10^{-11}$	$2.04 \times 10^8$
35	0	164	0	$1.50 \times 10^{-10}$	$8.66 \times 10^7$
70	0	159	0	$3.61 \times 10^{-10}$	$3.60 \times 10^7$
105	0	155	0	$8.9 \times 10^{-10}$	$1.46 \times 10^7$
140	0	151	0	$2.25 \times 10^{-9}$	$5.78 \times 10^6$
175	0	146	0	$5.83 \times 10^{-9}$	$2.23 \times 10^6$
210	0	141	0	$1.56 \times 10^{-8}$	$8.34 \times 10^5$
245	0	138	0	$4.29 \times 10^{-8}$	$3.03 \times 10^5$
	50	137	0.2	$1.36 \times 10^{-7}$	$9.59 \times 10^4$
	150	134	0.6	$3.64 \times 10^{-6}$	$3.58 \times 10^3$
	250	132	1	inf	0
280	0	133	0	$1.22 \times 10^{-7}$	$1.07 \times 10^5$
	50	131	0.2	$5.96 \times 10^{-7}$	$2.18 \times 10^4$
	150	125	0.6	$3.82 \times 10^{-5}$	$3.40 \times 10^2$
	250	120	1	inf	0
315	0	129	0	$3.59 \times 10^{-7}$	$3.62 \times 10^4$
	50	125	0.2	$2.71 \times 10^{-6}$	$4.79 \times 10^3$

	150	116	0.6	$4.16 \times 10^{-4}$	$3.13 \times 10^1$
	250	109	1	inf	0
350	0	125	0	$1.10 \times 10^{-6}$	$1.19 \times 10^4$
	50	119	0.2	$1.28 \times 10^{-5}$	$1.02 \times 10^3$
	150	108	0.6	$4.69 \times 10^{-3}$	2.77
	250	98	1	inf	0

As expected, the remaining failure life predicted in absence of cavities in Table 6 is higher than the value calculated with the effect of creep cavitation. A graphic representation with lines of the hardness values collected in Table 6 is presented in Figure 13(a) as function of service time together with the measures of hardness taken from field inspection at a certain replica level shown with points. The reference critical replica level is set at 250 cavities/mm<sup>2</sup>. The effect of changing the critical cavity level on the rupture time is represented in Figure 13(b) for three cavity levels from 250 to 500 cavities/mm<sup>2</sup>.

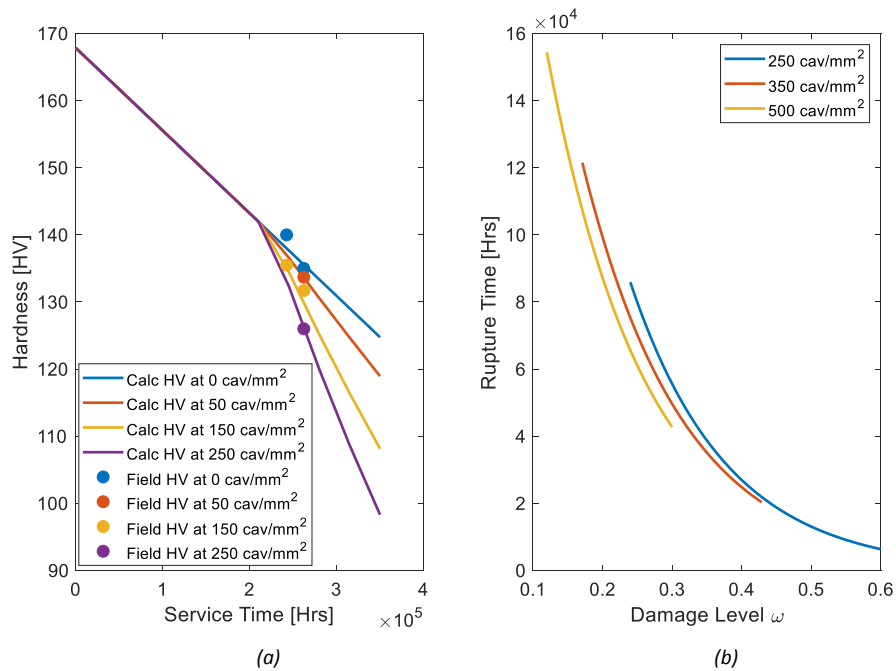


Figure 13: (a) Estimated and field Hardness variation as function of service time, and (b) Rupture time variation as function of damage level for different critical cavity levels.

A scenario that can be envisaged for practical power plant inspections is shown below as the station approaches end of life. This illustrates the periodic outage data capture and re-assessment process that would be applied in practice to inform decisions based on observed cavity counts. Table 7 illustrates the proposed approach, with the critical cavity density level being reassessed and reset at the last inspection point.

Table 7: Application of the new approach during inspections

Service Hours at Inspection Point [hrs]	HV	Cavity Density [cavities/mm <sup>2</sup> ]	$\omega$	Strain Rate [1/hrs]	$t_r$ [hrs]	Critical Cavity Density [cavities/mm <sup>2</sup> ]
241,734	137	60	0.24	1.52E-07	87,106	250
253,734	134.2	80	0.32	4.67E-07	27,840	250

259,734	132.6	90	0.36	8.76E-07	14,850	250
265,734	130.5	110	0.44	2.51E-06	5,174	250
265,734	130.5	110	0.338	1.29E-06	11,530	350

The average creep strain rate calculated from diametral strain measurements across installed creep pips for a period until 241,734 hrs on the main steam pipework has been reported from site diametral surveys to be in the order of  $3.173 \times 10^{-8} \text{ hrs}^{-1}$ , which gives a projected remaining life of 371 khrs. In this case the strain rates are estimated over different strain measurements samples taken at different operating periods allowing for the use of the Failure Forecast Method based on strain rate as a damage indicator [15]. The estimated remaining rupture time from eq. (27) in absence of cavities at 241,734 service hours is 333.4 khrs. The two values of remaining life calculated with the creep strain laws from Section 4.2.3 and the Failure Forecast Method are similar suggesting a good convergence of results in the absence of creep cavitation.

## 5. Discussion and Concluding Remarks

### 5.1 A Holistic Lifting Methodology

A hardness and creep replica assessment relationship has been quantified, for the first time, for parent material straight and bend sections using data extracted from in-service inspections on CrMoV material. This provides the capability to predict the residual life of ageing parent materials in service using a combination of hardness, surface replica data and strain, as illustrated in Figure 12. In practice there is a need to compare different residual life predictions based on assessments of field inspection data [15] against other computational predictions based on component reference stress and online plant temperature and pressure data [7].

The empirical solutions for the creep strain rate calculated from eqs. (26) and (28) through the integration with online (stress and temperature) and offline (hardness and replication) data show a good predictive capability and agree well with the strain rate values calculated from field measurements in Section 4.4. The creep rupture life is thus predicted suitably through its relationship with the creep strain rate. The master eqs. (18) and (22) that describe the straight and bend pipes behaviour allow the estimation of the strain rate with the advantage of providing a better comprehension of the in-service evolution of the failure mechanism that characterizes the material under investigation. Hardness and creep replica data must be used in conjunction for a correct projection of the material microstructure evolution and for the estimation of the strain rate and remaining life.

The approach takes account of the initial effect of thermal softening (hardness reduction in region 1) and creep damage (accelerated hardness reduction in region 2) illustrated by the hardness and creep cavity behaviour; Figure 8 for straight pipe sections. As material ages in service, the model can be further tuned by comparison between the estimated and measured value of hardness. Once the model is finely tuned, the field hardness measure will allow a more reliable estimation of creep cavities and consequently of creep strain rate. The examples presented in Section 4.4 illustrate this concept.

### 5.2 Industrial Significance

The approach developed in this paper complements the real decision-making process on an operating station, which considers all relevant data before making significant run-repair-replace decisions. The capability to detect the acceleration in damage is particularly important for the plant operator, since this acceleration is invariably the key behaviour that focusses attention and prompts decisions.

Currently hardness and surface replica data are not routinely used in predictive residual life models. The baseline inspection data used to develop the models for parent CrMoV has been acquired by very experienced inspection teams on ageing plant across multiple operating units, hence the quality is considered representative of good practice.

The assessment reveals definite trends in the population statistics for hardness data as plant ages, however the trends are less evident for the surface replica inspection data. It should be noted that the expected change in replica cavity count as the material ages has been affected by the sites' very conservative decision for wholesale pipework replacements on the inspected units. Other studies [2, 3] of ex-service CrMoV specimens extracted from the same pipework systems have confirmed that the decision to replace the pipework was very conservative.

### 5.3 Capabilities and Further Development

The models developed in this research illustrate the potential to better utilise existing inspection data for predictions of residual creep life. This innovation is even more powerful if it is complemented by, or integrated with, more sophisticated computational life assessment models that can efficiently account for the stress state in components and interpret the nuances associated with real plant operation [15].

The predictive capability and the accuracy of the empirical relationships proposed in this paper will improve with access to more field data, spread over longer operational periods. The new predictive models developed in this study show the potential future direction; for example in combination with a neural network approach [29] to efficiently determine the stress state and integrated with online monitor data.

### Acknowledgments

This work was supported by the Engineering and Physical Sciences Research Council, EPSRC (UK) (Grant number: EP/G037345/1). The funding is provided through the EPSRC Centre for Doctoral Training in Carbon Capture and Storage and Cleaner Fossil Energy ([www.ccsfce-cdt.ac.uk](http://www.ccsfce-cdt.ac.uk)). The work was also partly sponsored by the EDF Energy (UK). This support is gratefully acknowledged. The authors would also like to acknowledge EDF for permission to publish this paper.

### Data availability statement

The raw/processed data required to reproduce these findings cannot be shared at this time as the data also forms part of an ongoing study.

### References

- [1] A. Morris, B. Cacciapuoti, and W. Sun, "The role of hardness on condition monitoring and lifing for high temperature power plant structural risk management," *Measurement*, vol. 131, pp. 501-512, 2019/01/01/ 2019. DOI: <https://doi.org/10.1016/j.measurement.2018.09.002>.
- [2] B. Cacciapuoti, A. Morris, W. Sun, D. G. McCartney, and J. Hulance, "Correlation and capability of using site inspection data and small specimen creep testing for a service-exposed CrMoV pipe section," *Materials at High Temperatures*, vol. 36, no. 2, pp. 173-186, 2019/03/04 2019. DOI: <https://doi.org/10.1080/09603409.2018.1503148>.
- [3] M. Ejaz, "Creep Life Prediction of New and Service Exposed 0.5Cr0.5Mo0.25V Steel Pipework," PhD Thesis, Imperial College of London, 2019.
- [4] D. R. Barraclough, C. D. Hamm, and B. Plastow, "Creep Rupture Equations of Steels for use in Life Assessment Calculations based in ISO (1978) data," ed: CEBG publication NWR/SSD/84/006/R.
- [5] "European Creep Collaborative Committee, ECCC data sheets for steel."
- [6] B. S. Institution, "Elevated Temperature Properties for Steels for Pressure Purposes," PD 6525:Part 1: 1990.
- [7] A. Morris, B. Cacciapuoti, and W. Sun, "The role of small specimen creep testing within a life assessment framework for high temperature power plant," *International Materials Reviews*, vol. 63, no. 2, pp. 102-137, 2018/02/17 2018. DOI: <https://doi.org/10.1080/09506608.2017.1332538>.

- [8] B. R. Cardoso, C. F. T. Matt, H. C. Furtado, and L. H. De Almeida, "Creep Damage Evaluation in High-Pressure Rotor Based on Hardness Measurement," *Journal of Materials Engineering and Performance*, vol. 24, no. 7, pp. 2784-2791, 2015/07/01 2015. DOI: <https://doi.org/10.1007/s11665-015-1555-5>.
- [9] F. Masuyama, "Hardness model for creep-life assessment of high-strength martensitic steels," *Materials Science and Engineering: A*, vol. 510-511, pp. 154-157, 2009/06/15/ 2009. DOI: <https://doi.org/10.1016/j.msea.2008.04.133>.
- [10] B. Neubauer, "Remaining-life estimation for high-temperature materials under creep load by replicas," *Nuclear technology*, vol. 66, no. 2, pp. 308-312, 1984. DOI: <https://doi.org/10.13182/NT84-A33434>.
- [11] CEGB, "Creep life assessment of boiler pressure parts using strain data," *Report NWR/SSD/85/0031/R*, 1985.
- [12] B. J. Cane, "Remaining creep life estimation by strain assessment on plant," *International Journal of Pressure Vessels and Piping*, vol. 10, no. 1, pp. 11-30, 1982/01/01/ 1982. DOI: [https://doi.org/10.1016/0308-0161\(82\)90023-0](https://doi.org/10.1016/0308-0161(82)90023-0).
- [13] J. A. Williams and M. C. Coleman, "Application of current strain based remanent life models to real components " *CEGB TPRD/M/1277/N82*, 1982.
- [14] M. Prager, "Development of the MPC Omega Method for Life Assessment in the Creep Range," *Journal of Pressure Vessel Technology*, vol. 117, no. 2, pp. 95-103, 1995. DOI: <https://doi.org/10.1115/1.2842111>.
- [15] R. Bonetti, A. Morris, P. Shipway, and W. Sun, "Requirements for developing high temperature creep life models for ageing pipework systems using power plant condition monitoring and inspection data," *International Journal of Pressure Vessels and Piping*, vol. 188, p. 104233, 2020. DOI: <https://doi.org/10.1016/j.ijpvp.2020.104233>.
- [16] J. Corcoran and C. M. Davies, "Monitoring power-law creep using the Failure Forecast Method," *International Journal of Mechanical Sciences*, vol. 140, pp. 179-188, 2018/05/01/ 2018. DOI: <https://doi.org/10.1016/j.ijmecsci.2018.02.041>.
- [17] B. J. Cane, P. F. Aplin, and J. M. Brear, "A Mechanistic Approach to Remanent Creep Life Assessment of Low Alloy Ferritic Components Based on Hardness Measurements," *Journal of Pressure Vessel Technology*, vol. 107, no. 3, pp. 295-300, 1985. DOI: <https://doi.org/10.1115/1.3264453>.
- [18] S. Concari, "Residual life assessment and microstructure," *ECCC recommendations*, vol. 6, no. 1, pp. 1-30, 2005.
- [19] F. Masuyama, "Creep degradation in welds of Mod.9Cr-1Mo steel," *International Journal of Pressure Vessels and Piping* vol. 83, pp. 819-825, 11/01 2006. DOI: <https://doi.org/10.1016/j.ijpvp.2006.08.010>.
- [20] N. Saito, K. Ishiyama, T. Yamaguchi, and F. Masuyama, "Effect of Creep Degradation on Hardness Changes of Ni-based Alloys for A-USC Power Boiler," *ISIJ International*, vol. 59, no. 9, pp. 1695-1704, 2019. DOI: <https://doi.org/10.2355/isijinternational.ISIJINT-2018-878>.
- [21] D. J. Allen and S. T. Fenton, "A hardness-based creep rupture model for new and service aged P91 steel," in *VTT symposium*, 2007, vol. 246, p. 156: VTT; 1999Type of Work.
- [22] D. J. Allen, "GENSIP Grade 91 Good Practice Guide, Report R17 (GENSIP/R/PS027): A Hardness -Normalised Model Of Creep Rupture For P91 Steel," GENSIP2013.
- [23] M. Shammass, *Remanent Life Assessment of Ferritic Weld Heat Affected Zones by a Metallographic Measurement of Cavitation Damage: The 'A' Parameter*. Central Electricity Generating Board (CEGB) Technology Planning and Research Div, 1987.
- [24] R. Viswanathan, *Damage mechanisms and life assessment of high temperature components*. ASM international, 1989.

- [25] H. Riedel, "Life prediction methods for constrained grain boundary cavitation," *International journal of pressure vessels and piping*, vol. 39, no. 1-2, pp. 119-134, 1989. DOI: [https://doi.org/10.1016/0308-0161\(89\)90042-2](https://doi.org/10.1016/0308-0161(89)90042-2).
- [26] J. W. Wilson, D. J. Allen, A. J. Peyton, A. Shibli, and C. Davis, "Detection of creep degradation during pressure vessel testing using electromagnetic sensor technology," *Materials at High Temperatures*, vol. 34, no. 5-6, pp. 448-457, 2017. DOI: <https://doi.org/10.1080/09603409.2017.1375251>.
- [27] J. Corcoran, P. Hooper, C. Davies, P. B. Nagy, and P. Cawley, "Creep strain measurement using a potential drop technique," *International Journal of Mechanical Sciences*, vol. 110, pp. 190-200, 2016. DOI: <https://doi.org/10.1016/j.ijmecsci.2016.03.015>.
- [28] G. Sposito, C. Ward, P. Cawley, P. Nagy, and C. Scruby, "A review of non-destructive techniques for the detection of creep damage in power plant steels," *Ndt & E International*, vol. 43, no. 7, pp. 555-567, 2010. DOI: <https://doi.org/10.1016/j.ndteint.2010.05.012>.
- [29] J. Rouse, W. Sun, T. Hyde, A. Morris, and W. Montgomery, "A Method to Approximate the Steady-State Creep Response of Three-Dimensional Pipe Bend Finite Element Models Under Internal Pressure Loading Using Two-Dimensional Axisymmetric Models," *Journal of Pressure Vessel Technology*, vol. 136, p. 011402, 02/01 2013. DOI: <https://doi.org/10.1115/1.4025720>.
- [30] T. H. Hyde, A. A. Becker, W. Sun, and J. A. Williams, "Influence of geometry change on creep failure life of 90° pressurised pipe bends with no initial ovality," *International Journal of Pressure Vessels and Piping*, vol. 82, no. 7, pp. 509-516, 2005/07/01/ 2005. DOI: <https://doi.org/10.1016/j.ijpvp.2005.01.003>.
- [31] *Steel forgings for pressure purposes - Part 2: Ferritic and martensitic steels with specified elevated temperature properties*, BS EN 10222-2, 2000.
- [32] E. Pavlina and C. Van Tyne, "Correlation of yield strength and tensile strength with hardness for steels," *Journal of materials engineering and performance*, vol. 17, no. 6, pp. 888-893, 2008. DOI: <https://doi.org/10.1007/s11665-008-9225-5>.
- [33] J. Rouse, M. Leom, W. Sun, T. Hyde, and A. Morris, "Steady-state creep peak rupture stresses in 90° power plant pipe bends with manufacture induced cross-section dimension variations," *International Journal of Pressure Vessels and Piping*, vol. 105, pp. 1-11, 2013. DOI: <https://doi.org/10.1016/j.ijpvp.2013.02.002>.
- [34] A. Shibli, "7 - Boiler steels, damage mechanisms, inspection and life assessment," in *Power Plant Life Management and Performance Improvement*, J. E. Oakey, Ed.: Woodhead Publishing, 2011, pp. 272-303.
- [35] J. Dobrzański, A. Hernas, and G. Moskal, "6 - Microstructural degradation in boiler steels: materials developments, properties and assessment," in *Power Plant Life Management and Performance Improvement*, J. E. Oakey, Ed.: Woodhead Publishing, 2011, pp. 222-271.
- [36] R. Raj, "Nucleation of cavities at second phase particles in grain boundaries," *Acta Metallurgica*, vol. 26, no. 6, pp. 995-1006, 1978. DOI: [https://doi.org/10.1016/0001-6160\(78\)90050-0](https://doi.org/10.1016/0001-6160(78)90050-0).
- [37] M. Kassner and T. Hayes, "Creep cavitation in metals," *International Journal of Plasticity*, vol. 19, no. 10, pp. 1715-1748, 2003. DOI: [https://doi.org/10.1016/S0749-6419\(02\)00111-0](https://doi.org/10.1016/S0749-6419(02)00111-0).
- [38] B. Wilshire and A. Battenbough, "Creep and creep fracture of polycrystalline copper," *Materials science and engineering: A*, vol. 443, no. 1-2, pp. 156-166, 2007. DOI: <https://doi.org/10.1016/j.msea.2006.08.094>.
- [39] B. Dyson, "Use of CDM in materials modeling and component creep life prediction," *J. Pressure Vessel Technol.*, vol. 122, no. 3, pp. 281-296, 2000. DOI: <https://doi.org/10.1115/1.556185>.

- [40] U. F. Kocks, "A statistical theory of flow stress and work-hardening," *The Philosophical Magazine: A Journal of Theoretical Experimental and Applied Physics*, vol. 13, no. 123, pp. 541-566, 1966/03/01 1966. DOI: <https://doi.org/10.1080/14786436608212647>.
- [41] J. Rouse, W. Sun, T. Hyde, and A. Morris, "Comparative assessment of several creep damage models for use in life prediction," *International Journal of Pressure Vessels and Piping*, vol. 108, pp. 81-87, 2013. DOI: <https://doi.org/10.1016/j.ijpvp.2013.04.012>.
- [42] Y. Liu and S. Murakami, "Damage localization of conventional creep damage models and proposition of a new model for creep damage analysis," *JSME International journal series A solid mechanics and material engineering*, vol. 41, no. 1, pp. 57-65, 1998. DOI: <https://doi.org/10.1299/jsmea.41.57>.
- [43] L. Kachnov, "Time of the rupture process under creep conditions," *Izv. Akad. Nauk, USSR, Otd. Tekh. Nauk*, pp. 26-31, 1958. DOI: <https://ci.nii.ac.jp/naid/10030415483/en/>.
- [44] J.-L. Chaboche, "Continuum damage mechanics: Part I—General concepts," 1988. DOI: <https://doi.org/10.1115/1.3173661>.
- [45] Y. N. Rabotnov, "Creep problems in structural members," 1969. DOI: <https://doi.org/10.1115/1.3408479>.
- [46] J. Lemaitre, "A continuous damage mechanics model for ductile fracture," 1985. DOI: <https://doi.org/10.1115/1.3225775>.
- [47] K. R. Williams and B. Wilshire, "Effects of microstructural instability on the creep and fracture behaviour of ferritic steels," *Materials Science and Engineering*, vol. 28, no. 2, pp. 289-296, 1977/05/01/ 1977. DOI: [https://doi.org/10.1016/0025-5416\(77\)90183-5](https://doi.org/10.1016/0025-5416(77)90183-5).